Searching for localized cosmic particle sources with an unbinned maximum likelihood approach

Till Neunhöffer

Institute of Physics, University of Mainz, Staudinger Weg 7, 55099 Mainz, Germany

Abstract

An unbinned method to search for localized cosmic particle sources is presented. The expected source shape, the measured background shape, and the estimated angular resolution of individual tracks are used to construct a likelihood function. Estimates of the flux, the positition and - in particular - the significance of a source can be readily obtained. A full confidence belt construction to deduce flux limits is presented. General statistical issues when searching for sources of unknown position are discussed.

Key words: point source search, likelihood analysis, neutrino telescopes
PACS: 07.05.Kf, 95.55.Vj, 96.40.Tv

1 Introduction

This paper describes a procedure to search for localized cosmic particle sources in a given set of events. The procedure will be discussed in the context of a neutrino point source search done with a neutrino telescope stationed at the geographic South Pole (AMANDA [3] and IceCube [1]). Modifications to either search for extended objects or to use neutrino or cosmic ray experiments at other locations should be straight forward.

The discussion is limited to the case of only one source in the field of view of the detector, the flux and position of which is to be determined. Again extensions to more complicated cases should not be problematic.

In contrast to the standard *binned search* used in the field ([2]), the method presented does not use a search grid on the sky. Hence it does not suffer from efficiency

Email address: Till.Neunhoeffer@uni-mainz.de (Till Neunhöffer).

losses due to the bin size or a fixed search grid. An unbinned search tremendously improves the accuracy of the measurement of the source position.

In addition, the method introduces an elegant way to weight single events depending on individual properties, which is impossible in a binned approach, where an event is either *inside* or *outside* a predefined search bin. That makes it possible to make use of information in addition to the mere direction like the reconstructed energy or the angular resolution of an event.

The paper is organized as follows. First it discusses the information being used as input (section 2). This includes the construction of functions that describe the assumed signal and measured background shapes. In section 3 the likelihood function is constructed and the statistical estimates for source flux, source location, and significance $\hat{\zeta}$ are obtained. The latter is discussed in some detail in section 4. Section 5 shows an example for a significance estimate with and without a source present. Using $\hat{\zeta}$ as a measured quantity, section 6 details the construction of confidence plots to arrive at flux limits. Section 7 discusses the accuracy of the source position measurement. Section 8 presents statistical issues and solution ansatzes associated with the search for cosmic particle sources of unknown location. The paper closes with a brief discussion (section 9).

2 Input

The data set this search method is applied to consists of a set of events. For each event only a limited set of properties is used, i.e. its direction represented by its declination $\delta \in [-90°, 90°]$ and its right ascension $\alpha \in [0\mathrm{h}, 24\mathrm{h}[$, and its angular resolution σ. This uncertainty in directional reconstruction is described by a two-dimensional Gaussian covariance matrix, corresponding to a $1\,\sigma$ confidence ellipse.

Next the normalized distributions of background events $\mathcal{B} = \mathcal{B}(\alpha, \delta)$ and signal events $\mathcal{S} = \mathcal{S}(\alpha, \delta, \sigma; \mathbf{x}_0)$ shall be constructed, with $\mathbf{x}_0$ describing the position of the source. The knowledge of these distributions is sufficient to arrive at a significance estimate. In order to obtain confidence limits on the flux, the respective confidence belts need to be constructed using a Monte Carlo simulation (see section 6). The required additional information is discussed in subsection 2.2.

The coordinate system appropriate for the background function corresponds to the surface of a sphere described by α, δ, as detailed above. For a localized source it is advisable to use *local* coordinates that describe the vicinity of the source accurately well, but avoid the pitfalls that come with curved surfaces. The system used has its origin at the assumed location of the source and neglects the curvature. This can be envisioned as approximating the surface of the sphere by a tangent plane. For small distances (up to $5°$ or $10°$) the introduced differences are negligable (less than

0.03% or 1.3%, respectively). As a convention, the vertical axes in the local systems are always chosen such that they point towards the North Pole.

2.1 Background and signal distributions

The background distribution is obtained from the data, based on the assumption that a possible signal is small in comparison and will not distort the background. Alternatively, particular areas of the sky that correspond to known sources or to the search region could be omitted when determining the background.

The signal distribution is a convolution of three functions describing the source extension, a possible distortion introduced by the messenger, and the detector resolution.

The appropriate coordinate system to carry out the convolution is a local system around the position of the source, as discussed at the beginning of this section [1] .

As the resolution is different for each event, so is the shape of the signal distribution.

Note that the convolution discribed above is only required in the case of the signal distribution. For the background the *measured* distribution is used, hence the convolution has already been carried out by nature.

2.2 Additional information

If one wants to *simulate* a set of events, some more information is required.

First the resolution distributions for signal and background need to be known. For the latter they can be obtained from the data, for the former one relies on Monte Carlo simulations. Due to the detector geometry, the resolution may depend on the direction of an event.

Next, the relation between an incident total (neutrino) signal flux Φ^{ν}_{sg} and a resulting number of detected events μ_{sg} observed during the livetime $\mathrm{T_L}$ must be known:

$$\mu_{\mathrm{sg}} = \Phi^{\nu}_{\mathrm{sg}} \cdot \bar{\mathrm{A}}^{\nu}_{\mathrm{eff}} \cdot \mathrm{T_L} \cdot \epsilon^{\mathrm{bin}} \qquad . \tag{1}$$

[1] Note that the local coordinate system attached to the source location and the one used to obtain the detector resolution confidence ellipse need not be identical, as the first corresponds to the tangent plane at the source and the second to the tangent plane at each respective event. In both cases the local vertical axes point towards the North Pole. Thus typically they will be connected by a rotation (and a translation due to the different origins).

The constant of proportionality $\bar{\mathrm{A}}_{\mathrm{eff}}^{\nu}$ is called energy-averaged effective area. It depends on the assumed energy spectrum and the direction (declination). A bin efficiency ϵ^{bin} has been added. For the method presented $\epsilon^{\mathrm{bin}} = 1$ in contrast to binned searches.

Last but not least the number of background events N_{bg} is needed. For each simulated set of events it is drawn from a Poisson distribution with an expectation value equal to the observed number of events in the data set under study.

2.3 The distributions used in this paper

All plots shown in this paper have been made using a toy Monte Carlo simulation, modelled to resemble AMANDA data as presented in [2].

For telescopes at the geographic South Pole all distributions are independent of right ascension. In particular, the background can be described by the histogram of declination values of the observed events. It can be smoothed by an appropriate fit function in order to minimize fluctuations [2] .

The search is restricted to a point source signal, represented by a delta distribution. In case of charged current ν_μ interactions, the messenger distortion is due to the angle between the incident muon neutrino and the muon direction of flight. For sake of simplicity, the messenger distortion is approximated as a spherically symmetric Gaussian. The detector resolution is derived for each reconstructed track individually (as detailed in [9]). The convolution discussed in section 2.1 corresponds to adding the respective covariance matrices.

The average number of background events is taken to be either $N_{\mathrm{bg}} = 700$ or $N_{\mathrm{bg}} = 3500$, corresponding to one year or five years of AMANDA data, respectively. Their declination distribution (over the Northern hemisphere, i.e. $\delta \geq 0^\circ$) is parameterized by a higher order polynomial (not shown).

The resolution functions for signal and background are taken to be identical. The error ellipses can be represented in several ways (see [9]). Here the parameters σ, which is connected to the area of the ellipse [3] , the excentricity of the ellipse ϵ and the angle α between major axis and right ascension are used.

Both σ and ϵ can be fit by a Moyal distribution

$$\mathrm{M}(x; m, s) = \frac{1}{\sqrt{2\pi}} \cdot e^{-\frac{1}{2}\left(\lambda + e^{-\lambda}\right)} \qquad \text{with} \qquad \lambda = \frac{x - m}{s} \qquad . \tag{2}$$

[2] Such a fit is only justified, if the selection criteria are continous functions of the declination.

[3] I.e. $\sigma = \sqrt{\sigma_1 \cdot \sigma_2}$, with σ_1 and σ_2 denoting the major and minor axes of the ellipse.

The values used are $m_\sigma = 1.81°$, $s_\sigma = 0.36°$ and $m_\epsilon = 1.22$, $s_\epsilon = 0.11$. The distribution of the angle α is parameterized by a polynomial.

3 The likelihood formula

The probability of an event to be a signal event corresponds to the (average) fraction of signal events in the total sample. The parameter describing this probability is denoted as s.

With x_0 describing the position of the source sought, the likelihood function for a single event of measured position x_i and error σ_i is:

$$\mathcal{L}_i(\mathrm{s}, x_0; x_i, \sigma_i) = \mathrm{s} \cdot \mathcal{S}(x_0; x_i, \sigma_i) + (1 - \mathrm{s}) \cdot \mathcal{B}(x_i) \qquad . \tag{3}$$

As in an ensemble all events are independent of each other, the combined likelihood function $\mathcal{L}(\mathrm{s}, x_0)$ is obtained by multiplication over all events N:

$$\mathcal{L}(\mathrm{s}, x_0) = \prod_i^N \mathcal{L}_i(\mathrm{s}, x_0; x_i, \sigma_i) \tag{4}$$

or

$$\log L = -\log \mathcal{L}(\mathrm{s}, x_0) = -\sum_i^N \log \mathcal{L}_i(\mathrm{s}, x_0; x_i, \sigma_i) \qquad . \tag{5}$$

The only free parameters of $\mathcal{L}$ and $\log L$ are x_0 and s, corresponding to the position and strength of the source.

3.1 Estimators

For each position x_0, the estimate $\hat{\mathrm{s}}$ for s is obtained as usual by demanding that

$$\frac{\partial \log L}{\partial \mathrm{s}} \stackrel{!}{=} 0 \qquad . \tag{6}$$

The mathematical structure of $\log L$ guarantees that such a minimum exists, if there is at least one event with $\mathcal{S} > \mathcal{B}$ and one event with $\mathcal{S} < \mathcal{B}$. That is due to $\log L$ being a polynomial of order N with $N - 1$ real zeroes (for a more detailed discussion see [8]). The case with $\mathcal{S} < \mathcal{B}$ for all events is technically troublesome and corresponds to no events being close to the signal hypothesis. This will be further discussed in section 4.

For the investigation of a well known source candidate at position x_0, this minimization is sufficient. If searching for a source of unknown position, one first carries out the minimization with respect to s for all x_0 and then considers the resulting

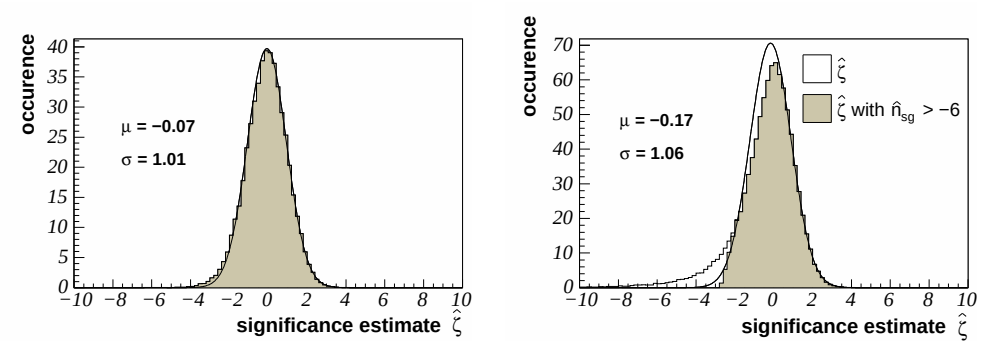

Figure 1. Distribution of the significance estimator at a declination of $\delta = 40°$ for the case of no signal source. For the left plot $N_{\mathrm{bg}} = 3500$ events and for the right plot $N_{\mathrm{bg}} = 700$ are distributed over the Northern hemisphere.

function $\log L(x_0, \hat{\mathrm{s}}(x_0))$. The most likely position of a source $\hat{x}_0$ is then at the extremum of this function with respect to x_0.

Multiplication of $\hat{\mathrm{s}}$ with N leads to an estimate for the number of signal events

$$\hat{n}_{\mathcal{S}} = \hat{\mathrm{s}} \cdot N \qquad , \tag{7}$$

which can by use of equation 1 be converted into a flux estimate $\hat{\Phi}_{\mathcal{S}}$.

The logarithmic likelihood function has another interesting property. The interval around its minimum, where the function value changes by 0.5, corresponds to the $1\,\sigma$ error - at least for the strictly Gaussian case. This can be used to control the uncertainty, when measuring the position of a source (see section 7). More importantly, it serves to construct an estimate for the significance of a detection

$$\hat{\zeta} = \frac{\hat{\mathrm{s}}}{\hat{\sigma}_{\hat{\mathrm{s}}}} \qquad . \tag{8}$$

Since the function $\log L(\mathrm{s})$ is known in its entirety, there are several ways to extract $\hat{\zeta}$. It has proven to be most robust to adjust a parabola with a minimum in $(\hat{\mathrm{s}}, \log L(\hat{\mathrm{s}}))$ and passing through $(0, \log L(0)$. This leads to

$$\hat{\zeta} = \mathrm{sign}(\hat{\mathrm{s}}) \sqrt{2 \cdot \ln \frac{\mathcal{L}(\hat{\mathrm{s}})}{\mathcal{L}(0)}} \qquad . \tag{9}$$

This quantity must not be confused with the so called *significance parameter* $\xi = -\log \mathcal{L}(\hat{\mathrm{s}})$ used elsewhere.

4 Significance properties

The construction of $\hat{\zeta}$ is based on a Gaussian assumption, which need not be correct a priori. For the example based on the distributions shown in section 2 with $N_{\mathrm{bg}} = 3500$ background events, this assumption is fully justified, as can be seen in figure 1 (left). The distribution of $\hat{\zeta}$ follows a Gaussian distribution centered around $\mu = 0$ with unit width ($\sigma = 1$), as expected for a significance.

The situation is more complicated, if there are fewer events in the data sample. This corresponds to a scenario where one cannot find an event in the vicinity of the assumed source position. In this case the calculation of $\hat{\zeta}$ returns too negative values for the significance. This is, however, not a real problem: if there are no events, then there is probably also no source.

Technically this feature needs to be controlled, though. The corresponding $\hat{\zeta}$ distribution is shown in figure 1 (right). For positive values of $\hat{\zeta}$ the curve is nicely Gaussian, as is indicated by an approriate fit [4]. The values outside the Gaussian fit are then identified by the cut $\hat{n}_S > -6$ (see eq. 7). Everytime this condition is violated, one instead uses $\hat{\zeta} = 0$, i.e. one conservatively sets the significance to zero.

This worsens the sensitivity by a few percent, but the situation is under control.

As soon as a simulated source signal is added, the $\hat{\zeta}$ distributions are well described by a Gaussian. The difficulty above doesn't arise, because usually there is an event close to the source hypothesis. The Gaussian nature is convenient to construct confidence plots. This will be discussed in section 6.

5 An example

Figure 2 shows an example from a toy Monte Carlo simulation to illustrate the presented technique. An area around the position of Markarian 421 ($\alpha = 11.07\,\mathrm{h}$, $\delta = 38.2°$) is displayed. All graphs show local $2\mathrm{h} \times 30°$ maps around the selected source position, as indicated on the left and the top of each figure. The dotted lines within the plots indicate lines of constant declination or right ascension, as indicated on the right and the bottom.

The two pictures on top represent the event positions. Figure 2 a) uses dots to indicate the positions only. This information is used in a binned search. A typical

[4] The integral of the fit is fixed to the integral of the histogram and then fit to the positive side of the curve.

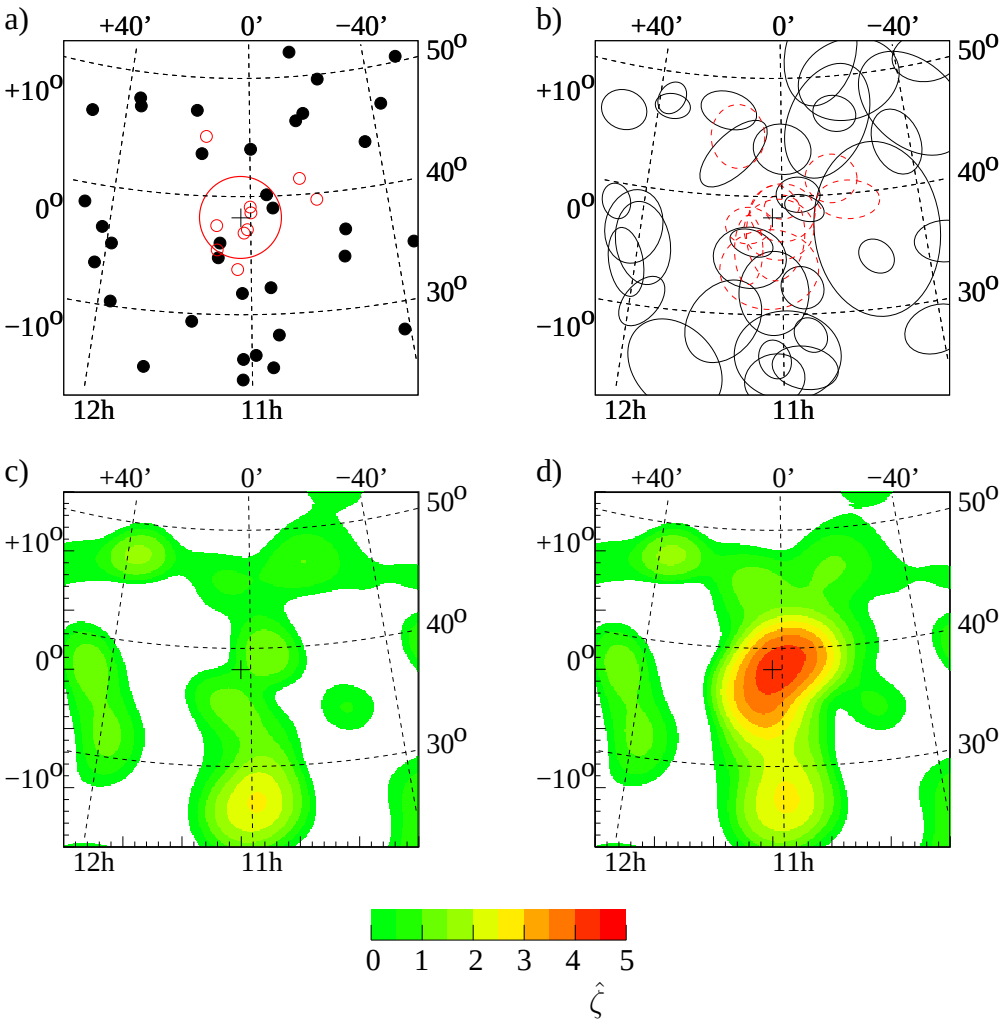

Figure 2. An example of the method showing event positions and significance estimates on a local map. See text.

search bin is depicted by the circle in the center of the graph. In Figure 2 b) the ellipses corresponding to the angular resolution are shown. Their information cannot be used by a binned approach.

On top of the background [5], ten signal events have been added. They are marked by the open/dashed symbols.

The two pictures in the lower row show the significance estimate $\hat{\zeta}$ without (Figure 2 c) and with added signal events (Figure 2 d) as a function of the source position hypothesis. Only values with $\hat{\zeta} \geq 0$ are shown. The source appears as a circular area with highest significance close to the true source position.

[5] Corresponding to $N_{\mathrm{bg}} = 700$ events in the whole Northern hemisphere

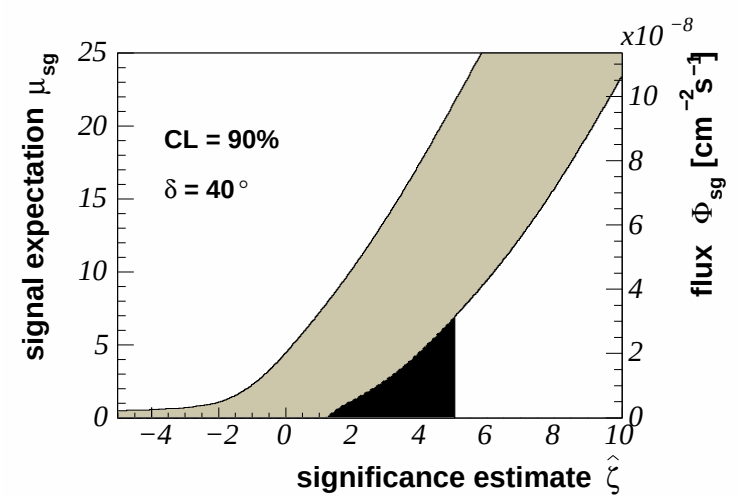

Figure 3. Example of a confidence plot constructed for a source declination of $\delta = 40°$ and 90% confidence level. On the horizontal axis $\hat{\zeta}$ is used as observable. On the vertical axis both the signal expectation $\mu_{\mathcal{S}}$ (left) and the signal flux $\Phi_{\mathcal{S}}$ (right) are shown. Since a discovery shall only be claimed if the 5σ lower boundary exceeds zero, an additional overcoverage has been introduced indicated by the dark shaded area.

The values at the source position x_0 are $\hat{\zeta} = 4.4$ and $\hat{\zeta} = 0.7$ for the cases with and without the additional signal, respectively.

6 Limits on the flux

The appropriate method to obtain limits on the signal flux is to construct confidence belts. The unknown but fixed parameter describing the signal can either be the expected number of signal events $\mu_{\mathcal{S}}$ or the signal flux $\Phi_{\mathcal{S}}$ itself. This is shown on the vertical axes in figure 3. The observable used on the horizontal axis is the significance estimate $\hat{\zeta}$ as defined by eq. 9.

As shown above, the $\hat{\zeta}$ distributions are Gaussian with their expectation values μ and their standard deviations σ being functions of $\mu_{\mathcal{S}}$. These functions have been evaluated for several fixed values of $\mu_{\mathcal{S}}$ and source declination values δ (see figure 4). They are well described by low order polynomials, so that values of $\mu_{\mathcal{S}}$ not explicitly simulated in the toy MC, can be interpolated.

With the $\hat{\zeta}$ distributions being well known for each value of $\mu_{\mathcal{S}}$ ($\Phi_{\mathcal{S}}$), the confidence belt construction can be carried out following the unified approach with likelihood ratio ordering ([5]) with the adaption that the width of Gaussian depends on the signal parameter. Figure 3 shows an example of a confidence plot such obtained.

The following comments can be made:

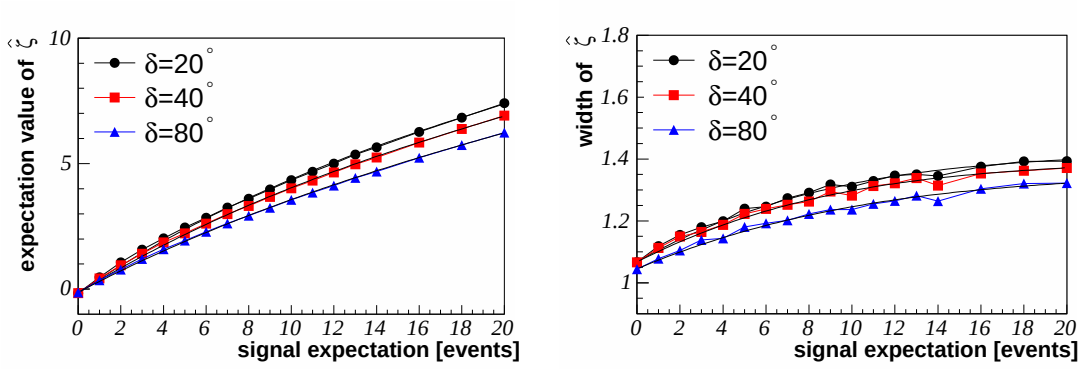

Figure 4. Mean μ and width σ of Gaussian fits to distributions of $\hat{\zeta}$ for different source declinations δ and different source strengths (expectation value $\mu_{\mathcal{S}}$). The markers indicate results of Monte Carlo simulations. The fits are second order polynomials. These graphs have been obtained within the simulation using $N_{\mathrm{bg}} = 700$ background events.

(1) The two quantities $\mu_{\mathcal{S}}$ and $\Phi_{\mathcal{S}}$ are proportional (see equation 1). The resulting confidence plot can thus be labeled twice on the y-axis, as is shown in the figure. Usually the effective area is not exactly known. The inclusion of the corresponding systematic uncertainty into the confidence belt construction is subject of ongoing research for the case of Poissonian statistics [4, 6]. The adaption to the Gaussian case should be straight forward.

(2) One would not announce a discovery if the lower limit at 90% confidence level exceeds zero. Rather one typically claims a discovery, if the $5\,\sigma$ lower boundary is positive. Then upper and lower limits at 90% CL can be quoted. This approach is indicated in figure 3. It corresponds to the artificial introduction of overcoverage as indicated in the graph.

(3) In the construction of the confidence belts above the observable $\hat{\zeta}$ is always taken at the same fixed source position x_0. If instead one searches in an extended area and uses e.g. the maximum value of $\hat{\zeta}$, the resulting distributions will be different and appropriate confidence plots need to be constructed. This will be discussed separately in section 8, as the problem is not specific to the search algorithm presented here.

(4) It should be emphasized that no simulations are necessary to arrive at the significance estimate $\hat{\zeta}$ itself, once the detector resolution and the messenger distortion are known. In contrast to flux limits, the significance can be obtained directly from the data.

7 Measuring the position of the source

The precision with which the position of a point source can be measured is limited by the width of the signal point spread shape $\mathcal{S}$. The precision improves with the number of signal events and it worsens with more background. If there were no

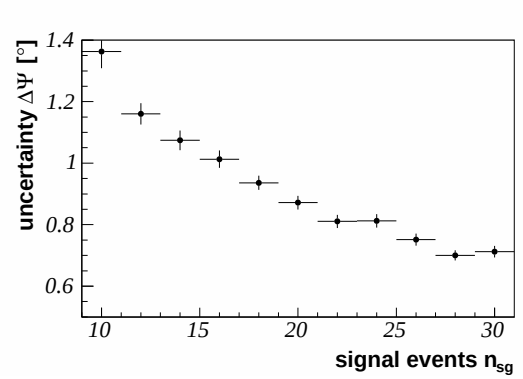

Figure 5. Accuracy of the position measurement as a function of the number of signal events. The example has been simulated for a source declination of $\delta = 40^\circ$. These results have to be compared to the assumed average resolution of a single event of approximately 2.3°.

background, the total signal resolution would approximately be $\sim \frac{1}{\sqrt{n}}\bar{\sigma}$. The fact, that there are events of different resolution in the sample improves this estimate, since those with better resolution receive a stronger than average weight.

For the example of section 2 (including background $N_{\mathrm{bg}} = 700$ events) figure 5 illustrates the uncertainty achieved with the likelihood method. In contrast to the binned search the uncertainty improves with the number of signal events. [6]

If investigating a source candidate another test option arises. Consider the case that one finds a significant excess *close* to the posititon of the source to be investigated. By studying the shape of the likelihood function around its minimum, it is possible to determine the probability that this excess is consistent with the assumed position x_0.

8 Searching in an area

This line of thought leads to the following interesting point. In the construction of the confidence plots in section 6, the observable $\hat{\zeta}$ is the significance estimate *at* the hypothesis position x_0. Another possible choice could have been the *maximum* significance in a certain (small) region *around* x_0. It is evident that the latter choice leads to systematically higher values. But for either case one can construct confidence belts and obtain comparable results for the flux limits.

For the search in a larger region of the sky - typically the complete field of view

[6] For the binned search the uncertainty of a position measurement is of the order of the radius of the bin. In the Gaussian case the three sigma ellipse contains 78% of all signal events. Therefore a typical bin radius is about three times as large as the typical resolution for a single event.

of the detector - the areas with the highest significance are of course those of most interest. A single observable that probes, whether a point source has been found, is the highest significance value $\hat{\zeta}_{\max}$ obtained over the whole search region. This variable has on average higher values than $\hat{\zeta}$, which corresponds to a single pre-selected source hypothesis position. Therefore it is necessary to construct new confidence plots for this particular observable.

With this demand a particular difficulty arises. The detector response usually differs for different source positions. This can e.g. be seen in Figure 4, where the expectation values and standard deviations of $\hat{\zeta}$ are plotted vs. the signal expectation. The fact that the three curves for the three different declinations are not identical shows the difference in detector response. Additionally, the interrelation of flux and signal expectation, i.e. the effective area, is direction dependent, too (eq. 1). This makes the construction of a single confidence plot with the flux (or the signal expectation) being the only parameter and $\hat{\zeta}_{\max}$ being the only observable impossible, because the knowledge of where the source is becomes a prerequisite to the construction of the plot. [7]

The general solution is to extend the confidence plot to also include the position of the source as a unkown parameter and the position of $\hat{\zeta}_{\max}$ as part of the observable. This ansatz is time consuming and a somewhat ardous task and has not been investigated in detail yet.

There are two special cases though, where this problem doesn't play a role. These will be discussed below.

8.1 Regions of uniform detector response

One can restrict the area to a region, where the detector response is uniform. In the case of AMANDA, this would correspond to azimuthal bands of fixed declination. Here confidence plots can be constructed in a straight forward manner. A source is placed at an arbitrary position to simulate the distributions for the case including signal for several fixed source fluxes.

An analytic expression to fit these distributions is obtained in the following way. Assume there were N source positions in the search area, with $\hat{\zeta}_j$ measured at each position, respectively. For now we neglect correlations between the $\hat{\zeta}_j$. The distribution of the significance estimates depending on the flux Φ is well known and denoted by $f(\hat{\zeta}, \Phi)$. Assume that only at one of these positions there truely is a

[7] This difficulty is not restricted to the specific choice of variable (i.e. $\hat{\zeta}_{\max}$) or even the search algorithm used, but remains present whenever the corresponding observables have different distributions for different source positions.

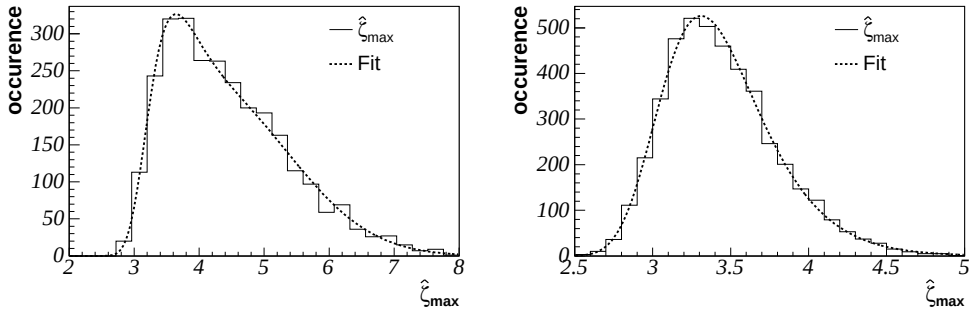

Figure 6. Distribution of highest significance as defined in equation 10 with signal source present (figure a) and without signal (figure b). In both graphs the histogram displays the simulated distribution. The continuous line shows a fit using equations 11 and 12, respectively.

source of strength Φ, whereas at the other positions there isn't. The observable

$$\hat{\zeta}_{\max} = \max_j(\hat{\zeta}_j) \tag{10}$$

in this case is given by the expression

$$\begin{aligned} f^N(\hat{\zeta}_{\max}) = f(\hat{\zeta}_{\max}, \Phi) \cdot \left(\int_{-\infty}^{\hat{\zeta}_{\max}} f(\hat{\zeta}, 0)\, \mathrm{d}\hat{\zeta} \right)^{N-1} \\ + (N-1) \cdot f(\hat{\zeta}_{\max}, 0) \cdot \int_{-\infty}^{\hat{\zeta}_{\max}} f(\hat{\zeta}, \Phi)\, \mathrm{d}\hat{\zeta} \left(\int_{-\infty}^{\hat{\zeta}_{\max}} f(\hat{\zeta}, 0)\, \mathrm{d}\hat{\zeta} \right)^{N-2} \end{aligned} \tag{11}$$

with the upper line of equation 11 describing the case, where $\hat{\zeta}_{\max}$ is actually obtained at the true position of the source and the lower line representing the possibility that the highest significance estimate $\hat{\zeta}_{\max}$ is measured at one of the other $(N-1)$ places.

For the case of no signal this expression simplifies to

$$f^N(\hat{\zeta}_{\max}, 0) = N \cdot f(\hat{\zeta}_{\max}, 0) \cdot \left(\int_{-\infty}^{\hat{\zeta}_{\max}} f(\hat{\zeta}, 0)\, \mathrm{d}\hat{\zeta} \right)^{N-1} \quad . \tag{12}$$

The assumption of uncorrelated measurements is wrong for neighboring search points, because $\hat{\zeta}$ forms a continuous function over the sky. Nevertheless equations 11 and 12 have successfully been used to describe AMANDA data, if the parameter N is being left free in the corresponding fit. One arrives at an *effective* number of search positions N_{eff}, which is roughly of the order of the search area divided by the size of a typical resolution ellipse.

A comparison of the simulated distribtion of $\hat{\zeta}$ with the analytic expressions of equations 11 and 12, respectively, are shown in figure 6. Both for the case including

a source (figure 6 a) and for the case of no signal (figure 6 b) the histograms can be well described by the models.

8.2 Investigating the significance only

Even in the case of non-uniform detector response to signal fluxes, the distribution of the significance estimate $\hat{\zeta}$ for the case of no signal is identical at all source positions by definition. It is a Gaussian of unit width centered around zero. This fact can be used to search for deviations from the background hypothesis. The distribution of the observable $\hat{\zeta}_{\max}$ follows equation 12. For any observed value of $\hat{\zeta}_{\max}$, the probability of it being a background fluctuation can be calculated.

Note though, that in this approach nothing can be said about the strength of a source so found [8]. Only the significance of the discovery can be measured. Nevertheless if one finds such a spot with extremely high significance in the dataset of a certain period of observation, one can then do a search at precicely this position in an independent dataset, e.g. that of the following year, with the confidence plot constructed as discussed in section 6 and so avoid the difficulties discussed in this section.

9 Discussion

The method described above has been tested with data from the AMANDA neutrino telescope. It has been applied to the same data set that serves for the limits presented in [2]. The resulting upper limits are compatible. Also the sensitivity, defined as the average upper limit in the case of no signal, is very similar in the two methods (for details see [8]).

Below we summarize the benefits and possible drawbacks of this unbinned maximum likelihood method.

9.1 Benefits of the method

(1) The precision to measure the position of a discovered source improves by about a factor of 4. Whereas in the binned search the uncertainty is of the order of the bin radius, it drops below the resolution for single events, as one would intuitively expect.

[8] The confidence plot constructed for the position, where $\hat{\zeta}_{\max}$ has been found, is not appropriate to be used, and the lower limit derived from it is systematically too high. Nevertheless, the upper limit is conservative.

(2) There is no arbitrary search grid involved. The bin efficiency is undesirable in the best case, where the bin is centered on a potential source. It worsens, if a source of unknown position is close to the border of bins in the search grid. With the maximum likelihood method a continous function over the sky is considered and the matter of bin efficiency is of no concern.
(3) The significance estimate $\hat{\zeta}$ is in itself a meaningful observable. In the binned search the number of events in the search bin serves as variable. This number becomes meaningful only with knowledge of the background expectation.
(4) The determination of $\hat{\zeta}$ is a very simple and robust process. No simulations are necessary. The only input are the data.
(5) The maximum likelihood approach makes it possible to make use of the resolution measurement for each event.
(6) It is also possible to include other per-event information in the likelihood construction. Most prominently the reconstructed energy of each event could be included.

9.2 Possible drawbacks of the method

(1) If flux limits are to be obtained, a (toy) Monte Carlo simulation is necessary, whereas in the binned search the distributions are Poissonian in nature and can hence be treated analytically. This especially influences the complexity of the optimization of quality criteria.
(2) Using additional information - such as the resolution estimation - can introduce additional systematics, if the determination of the resolution estimates is not absolutely correct.
(3) In areas of no events the significance estimate $\hat{\zeta}$ overestimates negative fluctuations. This effect and its remedy are discussed in section 4.
(4) The inclusion of systematic errors has yet to be done. Following the work done on Poissonian statistics ([4, 6]), this should not pose a problem.

9.3 Conclusion

The unbinned maximum likelihood method presented in this paper produces a robust significance estimate in a fast manner. The determination of flux limits relies on simulations, rather than pure analytic considerations. The method makes it possible to include angular resolution or other per-event information.

As the energy spectrum of a neutrino point source is expected to be much harder than the background of atmospheric neutrinos (see for example [7]), the inclusion of energy information should fairly improve the analysis power of the method.

When the first extraterrestrial sources are found, the likelihood mechanism will be used to measure their location with optimal precision.

Acknowledgements

I wish to thank the AMANDA collaboration for their support in obtaining the method described herein. I thank Lutz Köpke for many an illuminative and productive discussion. I would also like to thank the German Research Foundation (DFG) and the German Ministry of Education and Research (BMBF) for financial support of the AMANDA project.

References

[1] J. Ahrens et al. IceCube: The next generation neutrino telescope at the South Pole. *Nucl. Phys. Proc. Suppl.*, 118:388–395, 2003. astro-ph/0209556.

[2] J. Ahrens et al. Search for extraterrestrial point sources of neutrinos with AMANDA-II. *Phys. Rev. Lett.*, 92:071102, 2004.

[3] E. Andres et al. Observation of high-energy neutrinos using Cerenkov detectors embedded deep in Antarctic ice. *Nature*, 410:441–443, 2001.

[4] J. Conrad. *Search for Neutrinos from Cosmic Point Sources using AMANDA-B10 with Emphasis on Limit Calculation Techniques*. PhD thesis, Uppsala University, 2003.

[5] G. J. Feldman and R. D. Cousins. Unified approach to the classical statistical analysis of small signals. *Phys. Rev. D*, 57(7):3873–3889, 1998.

[6] G. C. Hill. Including Systematic Uncertainties in Confidence Interval Construction for Poisson Statistics. *Phys. Rev. D*, D67:118101, 2003.

[7] J. G. Learned and K. Mannheim. High-energy neutrino astrophysics. *Ann. Rev. Nucl. Part. Sci.*, 50:679–749, 2000.

[8] T. Neunhöffer. *Development of a new method to search for cosmic neutrino point sources with the AMANDA neutrino telescope*. Ph.D. thesis, University of Mainz, Germany, 2004. (Shaker Verlag, Aachen, ISBN 3-8322-2474-2, in German).

[9] T. Neunhöffer. Estimating the Angular Resolution of Tracks in Neutrino Telescopes based on a Likelihood Analysis. *Astropart. Phys.*, 2004. submitted, astro-ph/0403367.